Geochemistry Geophysics Geosystems G3

Article
Volume 13, Number 8
25 August 2012
Q08015, doi:10.1029/2012GC004135
ISSN: 1525-2027

Published by AGU and the Geochemical Society

Was the 1952 Tokachi-oki earthquake (*Mw* = 8.1) a typical underthrust earthquake?: Plate interface reflectivity measurement by an air gun–ocean bottom seismometer experiment in the Kuril Trench

Ryosuke Azuma, Yoshio Murai, Kei Katsumata, Yuichi Nishimura, and Takuji Yamada
Institute of Seismology and Volcanology, Hokkaido University, Sapporo 060-0810, Japan
(azuma@mail.sci.hokudai.ac.jp)

Kimihiro Mochizuki and Masanao Shinohara
Earthquake Research Institute, University of Tokyo, Tokyo 113-0032, Japan

[1] The Kuril Trench subduction zone is one of the most seismogenic regions, where underthrust earthquakes with $M > 8$ recur along the trench. The seismic gap between the source areas of the 1973 Nemuro-oki and 2003 Tokachi-oki earthquakes, which are typical underthrust earthquakes faulting with rupture velocities of ~3 km/s, has been ruptured by the 1952 Tokachi-oki earthquake. The seismic gap has also slipped incidental to neighboring asperities. The difference in slip pattern on the plate interface generally appears as a spatial difference in seismic structure on the plate interface, such as a reflectivity of the plate interface. We estimated the crustal velocity structure and analyzed the reflectivity of the plate interface to investigate the physical properties of the plate interface by performing an air gun–ocean bottom seismometer experiment on the along-trench profile across the seismic gap. Strong reflections from the plate interface were observed in the 1952 Tokachi-oki source area including the seismic gap, rather than in the 1973 Nemuro-oki source area. The strong reflectivity of the plate interface in such the seismic gap with an incidental slip suggests that a slip pattern in the corresponding seismic gap would be conditionally stable. The coupling condition in the source areas of the eastern part of the source area of the 1952 earthquake is different from that in source areas of typical underthrust earthquakes, such as the 2003 Tokachi-oki and 1973 Nemuro-oki earthquakes. Our results suggest that the 1952 Tokachi-oki earthquake was a complex earthquake with the characteristic of a tsunami earthquake.

Components: 5000 words, 5 figures.

Keywords: Kuril Trench; crustal structure; interplate reflectivity; seismic gap; tsunami earthquake; underthrust earthquakes.

Index Terms: 7230 Seismology: Seismicity and tectonics (1207, 1217, 1240, 1242); 7240 Seismology: Subduction zones (1207, 1219, 1240); 8150 Tectonophysics: Plate boundary: general (3040).

Received 7 March 2012; **Revised** 24 July 2012; **Accepted** 25 July 2012; **Published** 25 August 2012.

Azuma, R., Y. Murai, K. Katsumata, Y. Nishimura, T. Yamada, K. Mochizuki, and M. Shinohara (2012), Was the 1952 Tokachi-oki earthquake (*Mw* = 8.1) a typical underthrust earthquake?: Plate interface reflectivity measurement by an air gun–ocean bottom seismometer experiment in the Kuril Trench, *Geochem. Geophys. Geosyst.*, *13*, Q08015, doi:10.1029/2012GC004135.

1. Introduction

[2] The Kuril Trench subduction zone is one of the most seismogenic regions in the world. Typical underthrust earthquakes with rupture velocities of ~3 km/s [*Bilek*, 2010] occurred along this subduction zone, such as the 1843 Tokachi-oki ($M > 8$ [*Hatori*, 1984]), 1952 Tokachi-oki ($Mw = 8.1$ [*Hirata et al.*, 2003]), 1958 Etorofu-oki, 1963 Kuril Island and 1969 Kuril Islands ($Mw = 8.5$, 8.3, and 8.2, respectively [*Schwartz and Ruff*, 1987]), 1973 Nemuro-oki ($Mw = 7.8$ [*Yamanaka and Kikuchi*, 2002]), and the 2003 Tokachi-oki ($Mw = 8.0$ [*Yamanaka and Kikuchi*, 2003]) earthquakes. In this subduction zone, tsunami earthquakes, which generate unusually larger tsunami than that expected from their seismic waves, also occurred such as the largest aftershock of the 1963 Kuril earthquake. Those tsunami earthquakes rupture the plate interface very close to the trench with rupture velocities of ~1 km/s [*Pelayo and Wiens*, 1992; *Satake and Tanioka*, 1999]. We distinguish those tsunami earthquakes from typical underthrust earthquakes.

[3] The 1952 and 2003 Tokachi-oki earthquakes initiated the rupture from almost same place [*Yamanaka and Kikuchi*, 2003; *Hirata et al.*, 2003]. The source process analysis by using teleseismic body waves revealed that the 2003 Tokachi-oki earthquake, which is the latest large earthquake in the southern Kuril Trench, is a recurrent event of the 1952 Tokachi-oki earthquake [*Yamanaka and Kikuchi*, 2003]. However, the slip distribution of these two earthquakes deduced by tsunami waveform analysis differs from those by teleseismic wave analysis. Whereas the maximum coseismic slip of the 1952 earthquake distributed beneath Kushiro Canyon, which is located between the Tokachi-oki and Nemuro-oki segments, is more than 7 m [*Hirata et al.*, 2003], such a slip did not occur in 2003 [*Tanioka et al.*, 2004]. Therefore, the source areas of both earthquakes are significantly different. A comparison of the source areas of the 2003 Tokachi-oki and 1973 Nemuro-oki earthquakes estimated by *Yamanaka and Kikuchi* [2002, 2003] reveals a distinct seismic gap around Kushiro Canyon (Figure 1).

[4] We need to understand a coupling condition of plate interface in the seismic gap. Because the seismic gap has ruptured not independently but with neighboring asperities [*Satake and Yamaki*, 2005], we focused on the spatial variation of physical condition of the plate interface crossing over the seismic gap. One approach for estimating physical conditions is to investigate the spatial variation in the reflectivity of the plate interface, which reflects a physical property such as interplate coupling [*Fujie et al.*, 2002; *Mochizuki et al.*, 2005]. Strong reflectivity of the plate interface suggests a weak interplate coupling and a quasi-stable or aseismic slip condition in the corresponding area [*Mochizuki et al.*, 2005]. In contrast, weak reflectivity is mainly observed in an area with a large coseismic slip and indicates a strong coupling condition [*Sato et al.*, 2005; *Mochizuki et al.*, 2005].

[5] A giant tsunamigenic earthquake occurring with an interval of ~500 years was also detected and is believed to be the linking earthquake of the Tokachi-oki and Nemuro-oki segments [*Nanayama et al.*, 2003]. To understand the physical mechanism of the occurrence of such a disastrous link earthquake, it is crucial to study the relationship between the spatial variation of the interplate reflectivity around the seismic gap and the coseismic slip distribution along the southernmost Kuril Trench.

[6] An air gun–ocean bottom seismometer (OBS) experiment was conducted around the source area of the 1952 Tokachi-oki earthquake to investigate the variation of reflectivity of the plate interface suggesting the intensity of the interplate coupling. In this paper, we show the crustal image that includes reflectivity of the plate interface. We then discuss the significant variation in the reflectivity of the plate interface along the Kuril Trench and slip distributions of the 1952, 1973, and 2003 megathrust earthquakes.

2. Data Acquisition

[7] The air gun–OBS seismic experiment was conducted in August 2010 in cooperation with the multipurpose vessel Shinsei-maru (SNK OCEAN Co., Ltd.). The seismic line was parallel to the Kuril Trench axis and ran ~50 km landward from the trench axis with a length of ~240 km (Figure 1). The line passed over the source area of the 1952 Tokachi-oki and 1973 Nemuro-oki earthquakes. Twenty-one OBSs were deployed along this line with intervals of 10 km. An air gun array with a total volume of 50 L was used as a controlled source and was shot with an interval of ~220 m. In this study, 1036 traces were recorded by each OBS.

[8] Each OBS consisted of a 4.5 Hz three-component geophone. Air gun signals received at each OBS were recorded by using a recorder with a 16-bit A/D converter with a sampling rate of 128 Hz or a 24-bit A/D converter with a sampling rate of 200 Hz [e.g.,

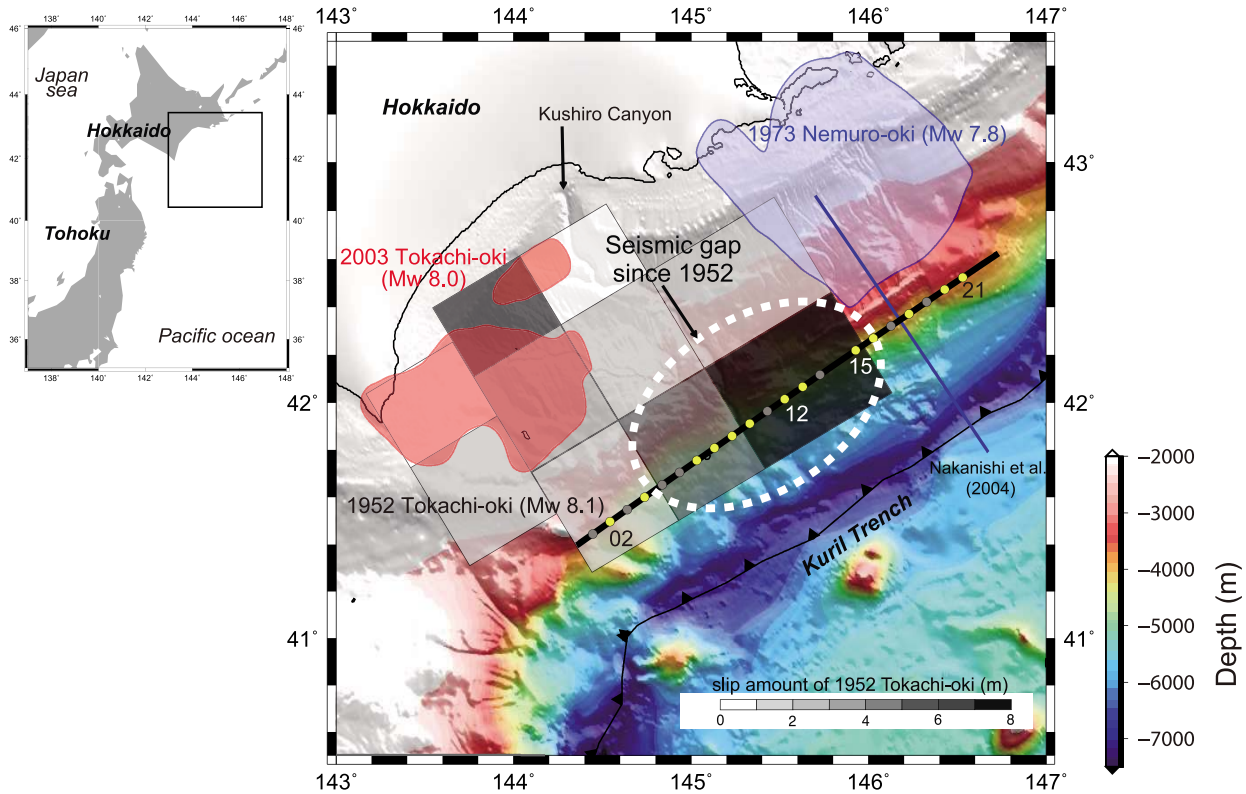

Figure 1. Map of seismic lines in the study area. Yellow circles denote the locations of the ocean bottom seismometers (OBSs) included in the analysis. Black and blue lines represent our seismic profile and that of *Nakanishi et al.* [2004], respectively. Areas in red and blue indicate slip areas of the 2003 Tokachi-oki and 1973 Nemuro-oki earthquakes, respectively [*Yamanaka and Kikuchi*, 2003, 2002]. Gray scale squares show the slip distribution of the 1952 Tokachi-oki earthquake (modified from *Hirata et al.* [2003]).

Shinohara et al., 2011, 2008; *Machida et al.*, 2009]. We estimated the accurate OBS positions on the sea bottom by obtaining arrival times of water waves within the offset range of 3 km from the OBS, applying the least square method. A band-pass filter of 4–13 Hz and a predictive error filter were applied. An amplitude gain control device was occasionally used for each waveform trace.

3. Traveltime Analysis

[9] We used *P* wave data recorded by the vertical component of 13 OBSs. From these data, we detected clear first arrivals within the source-receiver offset distance of 80 km, and their apparent velocity showed discontinuous jumps from 4.5 km/s to ~7 km/s around the offset distance of 40 km. Within this offset distance, the first arrival was observed continuously, and its apparent velocity gradually increased from 4.0 km/s to 4.5 km/s. However, no clear triplication was observed behind these first arrivals at all OBSs within corresponding offset distance (Figure 2). These results indicate that the *P* wave velocity (*Vp*) in the shallow part of the crustal structure gradually increases with depth without a velocity jump and the depth of the shallow boundary can hardly be constrained by using traveltimes of reflected waves. As a result, the velocity structure cannot be determined by forward modeling. In order to resolve this issue, we applied a tomographic traveltime inversion method for first arrival data [*Fujie et al.*, 2000].

[10] We first constructed a starting model for the traveltime inversion, which is represented by a uniform velocity gradient depending on depth. To recover the decreasing resolution with depth, we increased the grid interval with depth, from 1 km to 2 km for the depth grid and from 6 km to 15 km for the horizontal grid. The grid layout was set as 6 km × 1 km (horizontal × vertical) for depths of less than 6 km, 10 km × 2 km for depths of 6 km to 14 km, and 15 km × 2 km for depths of more than 14 km. We then reduced the effect of the shallow *Vp* structure on the inversion of far-offset

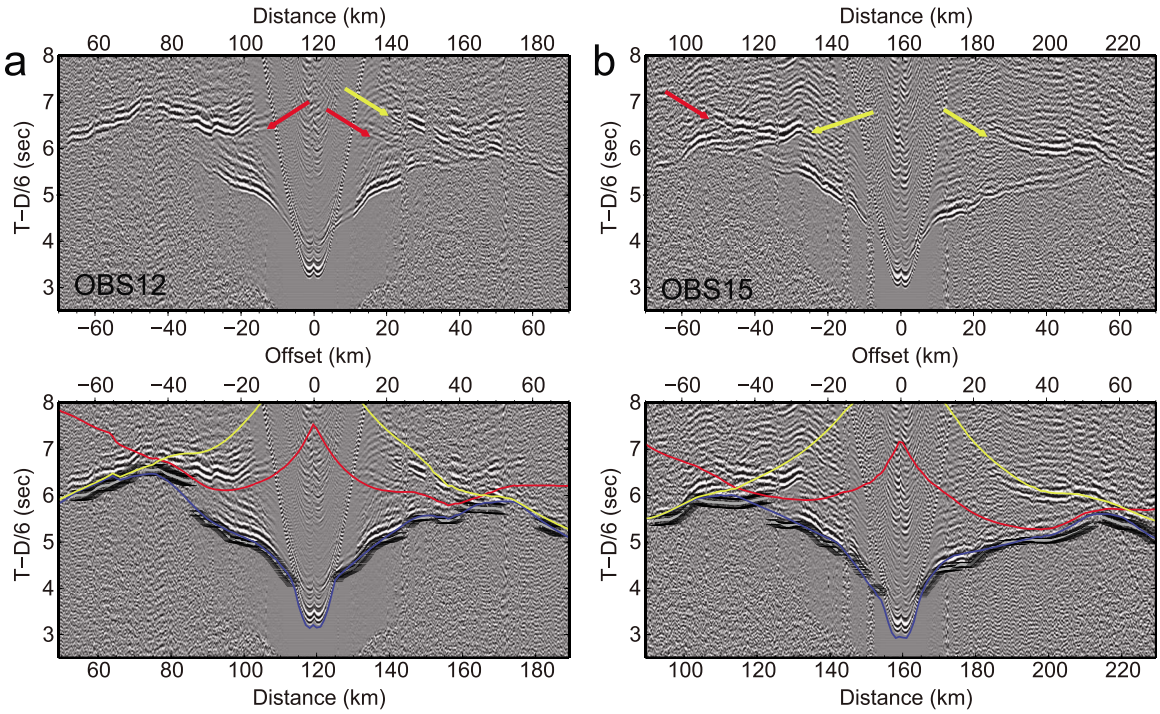

Figure 2. (top) Time-distance domain waveform data at (a) OBS12 and (b) OBS15. Red and yellow arrows indicate the phases reflected at the plate interface and the oceanic Moho, respectively. (bottom) Comparison of picked and synthetic first arrivals. The picked first arrivals are plotted by the black line with a pick uncertainty of ±50–100 ms. The blue line indicates the synthetic first arrival calculated from the final model illustrated in Figure 3. Red and yellow lines denote the calculated traveltime curves of reflected waves at the plate interface and the oceanic Moho, respectively, assuming depths of 14 km and 21 km, respectively (Figure 3).

traveltime by dividing the inversion process into two iteration steps. Data within an offset distance of less than 40 km were used in the first iteration, and the remaining offset data were used in the second iteration. Uncertainties of ±50 ms and ±100 ms were given to the first arrival with an apparent velocity of slower and faster than 5 km/s, respectively, considering the decrease of amplitude of waveforms due to attenuation with distance. We fixed these uncertainties during all iterations. The calculation in the second iteration began with the output model of the first iteration. In this manner, we succeeded in confining the short-wavelength heterogeneity in the traveltime data resulting from the shallow structure and in reducing the anomalous high/low velocities in the deep structure. As a result, we were able to estimate the *Vp* structure at all depths of less than ∼25 km (Figures 3 and 4).

[11] To obtain the reflectivity image, we used a traveltime mapping method (TMM) for traveltime data of reflected waves [*Fujie et al.*, 2006], which applies the diffraction stack type of wide-angle prestack migration [e.g., *Simon et al.*, 1996], after the velocity estimation. This method calculates a traveltime field from a velocity field and directly projects the observed reflection phases from the time-distance domain onto a depth-distance domain. Thus, the misidentification of later phases can be avoided and the phases can be evaluated objectively [*Fujie et al.*, 2006]. A clear reflection phase was detected 1.0–1.5 s later than the first arrival around offset distances of 25–60 km. An additional phase was evident ∼1.5 s later than the first arrival at the same offset. Uncertainty of traveltime pick with ±100 ms was given to all reflection phases, considering unclear arrivals due to the influence of the reverberation of the first arrival in addition to attenuation with distance. By using TMM, two reflectors were detected at the depth of 14 km as the former phase (shown by yellow arrows in Figure 2) and 20 km for the latter phase (shown by red arrows in Figure 2).

4. Results

[12] The final *Vp* model is shown in Figure 3. The resolution and ray distribution after the second

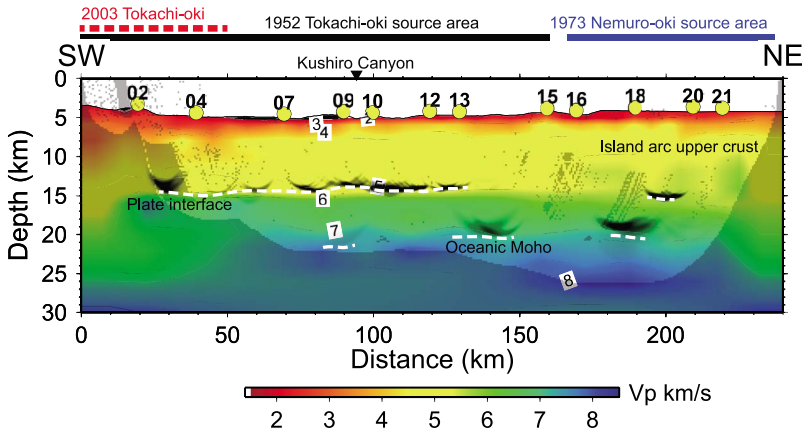

Figure 3. Final *P* wave velocity model. The ray is not distributed in the shadow area. The yellow plots show ocean bottom seismometer (OBS) positions along the profile. The source areas of the 1952 Tokachi-oki [*Hirata et al.*, 2003] and 1973 Nemuro-oki [*Yamanaka and Kikuchi*, 2003] earthquakes are represented by black and blue lines, respectively, above the model. The hyperbola-like shapes indicate reflection traveltime on the depth-distance domain, mapped by traveltime mapping method (TMM) [*Fujie et al.*, 2006].

iteration are shown in Figures 4a and 4b, respectively. Our inverse calculation showed good resolution, except in the depth range of 10–14 km (Figure 4a). The poorly resolved zone at depths of 10–14 km in the distance of 0–120 km would come from the lack of data due to the existence of traveltime jump of first arrivals, which is clearly evident in the waveforms from OBS02 to OBS12 (Figure 2a). Hereafter we call this zone as the shadow zone. In contrast, the traveltime jump of first arrivals observed at OBSs 02–12 was not recognized well at the western OBSs 13–21 (Figure 2b). The depths of 10–14 km in the distance of 120–200 km were resolved well (Figure 4a) because more raypaths can be calculated than those in the eastern side of the profile (Figure 4b). The root-mean-square of traveltime residuals decreased well from 4,319 ms to 104 ms during all inversion iterations. Although depths of greater than 10 km were poorly resolved, we were able to get the characteristics in *Vp* values.

[13] The *Vp* structure at depths of less than 8 km varied in the horizontal direction, indicating the thickness variation in the sedimentary layer. The thickest part at the distance of 0–80 km corresponds to the Tokachi-oki forearc basin [e.g., *Tsujino*, 2010]. At depths from ~7 km to ~14 km, which included the less resolved part, the structure had a *Vp* of 4–5 km/s. According to *Nakanishi et al.* [2004], this *Vp* value is typical for the island arc upper crust. The *Vp* increased considerably over 6 km/s at a depth of ~14 km, which is consistent with that of the plate interface in the model of *Nakanishi et al.* [2004]. A *Vp* of 6–7 km/s is roughly consistent with that of oceanic crust [e.g., *White et al.*, 1992; *Nakanishi et al.*, 2004]. The structure at depths of more than ~20 km had a *Vp* of

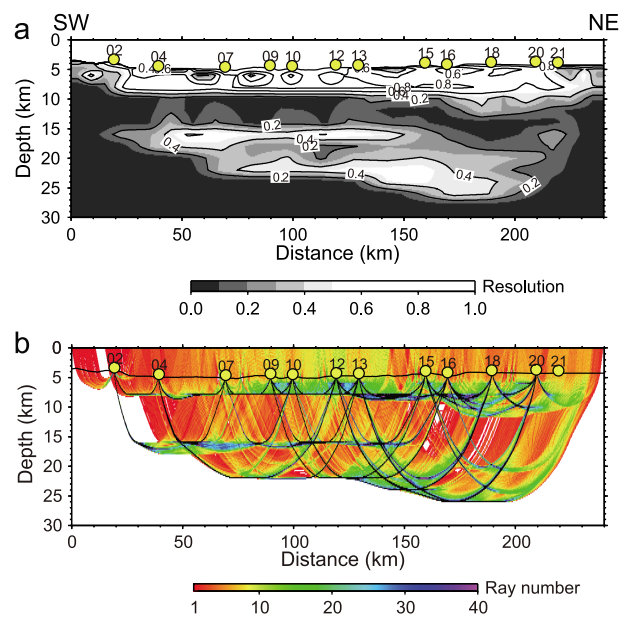

Figure 4. (a) Resolution of the final model illustrated in Figure 3. The gray scale represents the diagonal elements of the resolution matrix [*Fujie et al.*, 2000]. The bright areas are well resolved. Yellow circles indicate ocean bottom seismometer (OBS) positions along the profile. (b) Ray distribution of the inversion. Colors represent the number of rays. Yellow circles indicate OBS position along the profile.

~7.8 km/s, which is smaller than the *Vp* of the usual uppermost oceanic mantle [e.g., *White et al.*, 1992].

[14] Reflectors were distributed only in the deeper structure. As mentioned in the previous section, the amplitudes of reflected waves from the shallow structural boundary were too small to be picked (Figure 2). However, several phases with high amplitude were observed subsequent to the first arrival at the offset range of 25–60 km by OBSs mainly in the western half of the profile (Figure 2). One group, indicated by red arrows in Figure 2, was distributed at a depth of ~14 km as seen in Figure 3. From the comparison of the final *Vp* model to that of the Nemuro-oki region [*Nakanishi et al.*, 2004], the reflector can be interpreted as the plate interface (Figure 3). Similar reflection phases were indistinct from OBS15 to OBS21 (Figure 2b). Additional clear reflection phase, indicated by yellow arrows in Figure 2, was distributed at ~21 km and can be interpreted as the oceanic Moho (Figure 3).

5. Discussion

[15] The traveltime curves of first arrivals show a jump around the offset distance of 40 km in OBSs 02–12 deployed at the western half of the profile (Figure 2a). Moreover, the jump of first arrivals is not recognized well at OBSs 13–21 (Figure 2b). As compared to the *Vp* model for the Nemuro-oki region [*Nakanishi et al.*, 2004], the depth of the shadow zone in our *Vp* model (Figures 3 and 4b) corresponds to the lower part of the island arc upper crust. Observed traveltime jump of the first arrival indicates the existence of low velocity and/or reversed velocity gradients [e.g., *Takahashi et al.*, 2004]. In addition, the less resolved region due to the traveltime jump of the first arrival is exactly above the plate interface (Figures 3 and 4a). Therefore, the along-arc variation of the traveltime jump of the first arrival implies a variation in the thickness of a low velocity layer above the plate interface. Seismic experiments at the Japan Trench axial region detected the incoming sediment with a thickness of several kilometers in maximum beneath the island arc crust [*Tsuru et al.*, 2002]. Although we could not determine the accurate thickness and seismic velocity of that layer, the along-arc variation of the shadow zone indicates that the corresponding layer is qualitatively thinner in the Nemuro-oki segment than in the Tokachi-oki segment.

[16] The reflection of the plate interface was not observable in the source area of the 1973 Nemuro-oki earthquake [*Yamanaka and Kikuchi*, 2002]. *Nakanishi et al.* [2004] reported that the amplitude of the reflection from the plate interface was reduced at depths greater than ~15 km and that the less reflective area corresponded to the region of large slip in the 1973 event. Similar to *Nakanishi et al.* [2004], our result shows that low reflectivity appears to be a typical characteristic of large asperities on the plate interface.

[17] On the contrary, the section with strong reflectivity coincided with the seismic gap between the source areas of the 2003 Tokachi-oki and 1973 Nemuro-oki earthquakes (Figures 3 and 5a). A fluid-rich layer, such as that created by sediment entering the interplate, is generally apparent where the plate interface shows strong reflectivity [*Tsuru et al.*, 2005; *Floyd et al.*, 2001]. Under the condition of strong reflectivity, accumulation of shear stress at the plate interface does not occur as easy as at a typical plate interface [e.g., *Kasahara et al.*, 2003]. However, the seismic gap was ruptured during the 1952 earthquake [*Hirata et al.*, 2003]. The coseismic slip of the 2003 earthquake [*Tanioka et al.*, 2004; *Yamanaka and Kikuchi*, 2003] did not extend to the corresponding seismic gap (Figure 5a), nor did the large afterslip accompanying aftershocks [*Baba et al.*, 2006; *Miyazaki et al.*, 2004] (Figure 5b). The fact that strong reflectivity was observed at the plate interface with such complex slip characteristics suggests that the coseismic slip pattern in the corresponding area will be different from that of the 2003 and 1973 earthquakes, which were typical underthrust earthquakes [e.g., *Satake and Yamaki*, 2005; *Yamanaka and Kikuchi*, 2002, 2003; *Hatori*, 1974]. Therefore, characteristic of the plate interface in the seismic gap differs from that of the plate interface ruptured by typical underthrust earthquakes.

[18] Lateral variation of the interplate reflectivity suggests that the coupling condition in the seismic gap differs from that in a typical underthrust plane. The stress should be accumulated in the seismic gap where a coseismic slip of the 1952 earthquake occurred. The possibility of strong interplate coupling is supported by inland geodetic data, which showed a high slip-deficit rate at the source regions of Tokachi-oki and Nemuro-oki earthquakes [*Hashimoto et al.*, 2009]. Considering the strong reflectivity of the plate interface and interplate coupling in the seismic gap, the slip pattern would be conditionally stable; that is, neither seismic nor

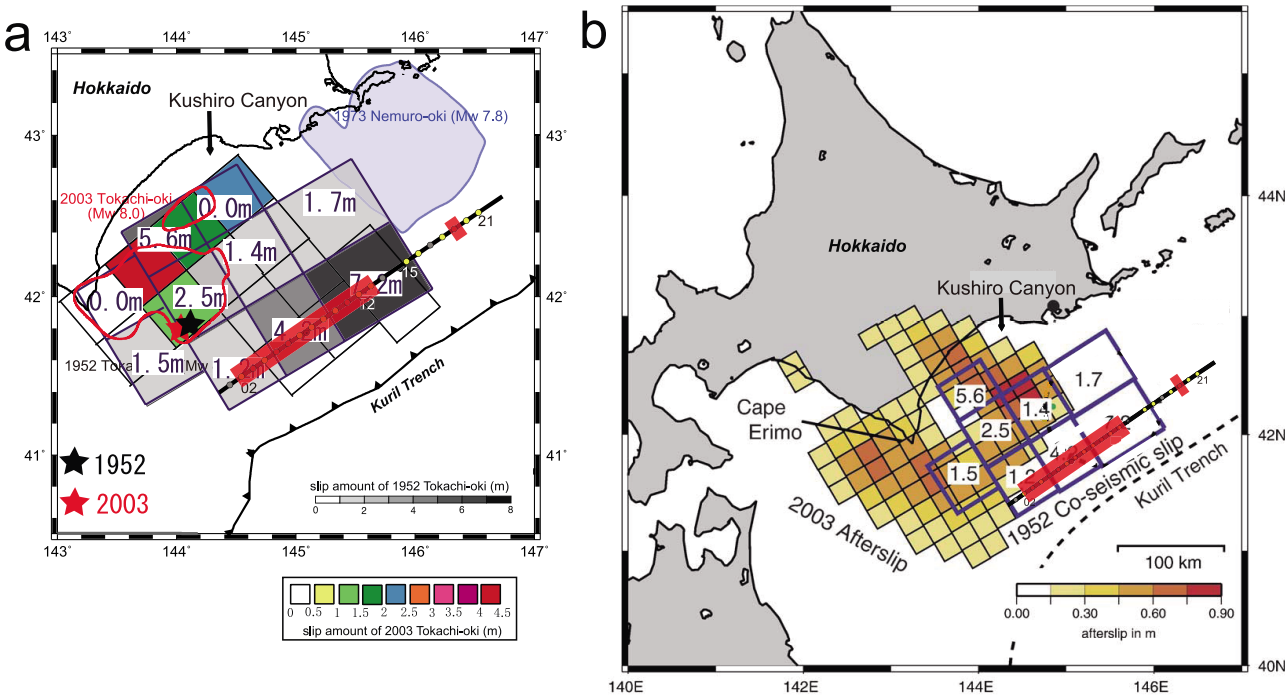

Figure 5. (a) Comparison between the reflectivity of plate interface and Tokachi-oki tsunami sources of the 1952 [*Hirata et al.*, 2003] and 2003 earthquakes [*Tanioka et al.*, 2004], modified from *Tanioka et al.* [2004]. The thick red line indicates the region of observed strong reflection. Slip amounts of the 1952 and 2003 events are shown by gray- and color-scale, respectively. Red and blue contours indicate slip areas of the 2003 Tokachi-oki [*Yamanaka and Kikuchi*, 2003] and 1973 Nemuro-oki earthquakes [*Yamanaka and Kikuchi*, 2002], respectively. (b) Comparison of the reflectivity of plate interface, afterslip of the 2003 Tokachi-oki earthquake, and tsunami source of the 1952 Tokachi-oki earthquake (modified from *Baba et al.* [2006]).

quasi-static slip would be evident. Therefore, the slip could have occurred at the seismic gap incidental to faulting at the Tokachi-oki and/or Nemuro-oki asperities [*Satake and Yamaki*, 2005]. Our result suggests that the seismic gap could have become an asperity with the potential to generate a giant tsunami near the trench axial region, such as that from the 1896 Sanriku earthquake, with a tsunami magnitude (*Mt*) of 8.2–8.6 [*Tanioka and Satake*, 1996; *Abe*, 1979], or the 2011 off Pacific coast of Tohoku earthquake (*Mw* = 9.0) [e.g., *Fujii et al.*, 2011; *Maeda et al.*, 2011; *Shinohara et al.*, 2011]. The 1896 Sanriku earthquake was a tsunami earthquake which generated unusually larger tsunami than that expected from its seismic waves [*Kanamori*, 1972; *Tanioka and Satake*, 1996; *Tanioka and Seno*, 2001]. The characteristic of the plate interface which was ruptured by this Sanriku tsunami earthquake can be similar to that of the seismic gap in this study. Therefore, our results suggest that the 1952 Tokachi-oki earthquake would have the characteristic of a tsunami earthquake in addition to that of a typical underthrust earthquake. Although further studies are necessary to investigate the triggering mechanism of the rupture of a conditional slip area, our result provides important information in understanding the occurrence mechanism of giant earthquakes with occurrence intervals of ~500 years [*Nanayama et al.*, 2003].

6. Conclusions

[19] We performed an air gun–OBS seismic experiment around the source area of the 1952 Tokachi-oki earthquake. The traveltime of the observed first arrivals was analyzed by first-arrival tomographic inversion. In addition, we applied TMM to the traveltime of the observed reflected waves.

[20] We estimated the *Vp* structure in the overriding island arc crust, subducted oceanic crust and uppermost mantle. TMM results showed strong reflectivity at the plate interface in the seismic gap that was ruptured only by the 1952 Tokachi-oki earthquake. The reflectivity was weak for the 1973 Nemuro-oki source area. Although strong reflectivity of the plate interface indicates that the area

would have slip in stable or quasi-static, we detected strong reflectivity in the seismic gap that slipped seismically in 1952. Considering the strong reflectivity and the past records of rupture in the seismic gap, the slip pattern in the seismic gap would be conditionally stable; that is, neither seismic nor quasi-static slip would be evident. Our results suggest that the 1952 Tokachi-oki earthquake was a complex one with the characteristic of a tsunami earthquake in addition to that of a typical underthrust earthquake. Although further studies are needed to investigate the triggering mechanism of rupture of a conditional slip area, our result provides important information in understanding the occurrence mechanism of giant earthquakes with intervals of ∼500 years.

Acknowledgments

[21] We thank the captain and crew aboard Shinsei-maru, SNK Ocean Co., Ltd., for their cooperation. The staff of Service Engineering Co., Ltd., provided support in the air gun operation. The air gun system was provided by ERI, University of Tokyo. We thank G. Fujie, R. Hino, T. Sato, H. Takahashi, and Y. Tanioka for their useful comments and suggestions. We used the wave analyzing tool PASTEUP and the velocity structural modeling editor MODELING [*Fujie et al.*, 2000]. All figures were prepared using Generic Mapping Tools (GMT) 4.5.3 [*Wessel and Smith*, 1991].

References

Abe, K. (1979), Size of great earthquakes of 1873–1974 inferred from tsunami data, *J. Geophys. Res.*, *84*(B4), 1561–1568, doi:10.1029/JB084iB04p01561.

Baba, T., K. Hirata, T. Hori, and H. Sakaguchi (2006), Offshore geodetic data conducive to estimation of the afterslip distribution following the 2003 Tokachi-oki earthquake, *Earth Planet. Sci. Lett.*, *241*, 281–292, doi:10.1016/j.epsl.2005.10.019.

Bilek, S. L. (2010), Invited review paper: Seismicity along the south American subduction zone: Review of large earthquakes, tsunamis, and subduction zone complexity, *Tectonophysics*, *495*, 2–14, doi:10.1016/j.tecto.2009.02.037.

Floyd, J. S., J. C. Mutter, A. M. Goodliffe, and B. Taylor (2001), Evidence for fault weakness and fluid flow within an active low-angle normal fault, *Nature*, *411*, 779–783, doi:10.1038/35081040.

Fujie, G., J. Kasahara, T. Sato, and K. Mochizuki (2000), Traveltime and raypath computation: A new method in a heterogeneous medium, *Geophys. Explor.*, *53*(1), 1–11.

Fujie, G., J. Kasahara, R. Hino, T. Sato, M. Shinohara, and K. Suyehiro (2002), A significant relation between seismic activities and reflection intensities in the Japan Trench region, *Geophys. Res. Lett.*, *29*(7), 1100, doi:10.1029/2001GL013764.

Fujie, G., A. Ito, S. Kodaira, N. Takahashi, and Y. Kaneda (2006), Confirming sharp bending of the Pacific Plate in the northern Japan trench subduction zone by applying a traveltime mapping method, *Phys. Earth Planet. Inter.*, *157*, 72–85, doi:10.1016/j.pepi.2006.03.013.

Fujii, Y., K. Satake, S. Sakai, M. Shinohara, and T. Kanazawa (2011), Tsunami source of the 2011 off the Pacific coast of Tohoku Earthquake, *Earth Planets Space*, *63*, 815–820, doi:10.5047/eps.2011.06.010.

Hashimoto, C., A. Noda, T. Sagiya, and M. Matsu'ura (2009), Interplate seismogenic zones along the Kuril-Japan trench inferred from GPS data inversion, *Nat. Geosci.*, *2*, 141–144, doi:10.1038/ngeo421.

Hatori, T. (1974), Source area of the tsunami off the Nemuro Peninsula in 1973 and its comparison with the tsunami in 1894 [in Japanese with English abstract and figure captions], *Bull. Earthquake. Res. Inst.*, *13*, 67–76.

Hatori, T. (1984), Source area of east Hokkaido tsunami generated in April, 1843 [in Japanese with English abstract and figure captions], *Bull. Earthquake Res. Inst.*, *59*, 423–431.

Hirata, K., E. Geist, K. Satake, Y. Tanioka, and S. Yamaki (2003), Slip distribution of the 1952 Tokachi-oki earthquake (*M* 8.1) along the Kuril Trench deduced from tsunami wave form inversion, *J. Geophys. Res.*, *108*(B4), 2196, doi:10.1029/2002JB001976.

Kanamori, H. (1972), Mechanism of tsunami earthquakes, *Phys. Earth Planet. Inter.*, *6*, 346–359, doi:10.1016/0031-9201(72)90058-1.

Kasahara, J., M. Toriumi, and K. Kawamura (2003), *Role of Water on Earthquake Generation* [in Japanese], 389 pp., Univ. of Tokyo Press, Tokyo.

Machida, Y., et al. (2009), Heterogeneous structure around the rupture area of the 2003 Tokachi-oki earthquake (*Mw* = 8.0), Japan, as revealed by aftershock observation using Ocean Bottom Seismometers, *Tectonophysics*, *465*, 164–176, doi:10.1016/j.tecto.2008.11.009.

Maeda, T., T. Furumura, S. Sakai, and M. Shinohara (2011), Significant tsunami observed at ocean-bottom pressure gauges during the 2011 off the Pacific coast of Tohoku Earthquake, *Earth Planets Space*, *63*, 803–808, doi:10.5047/eps.2011.06.005.

Miyazaki, S., P. Segall, J. Fukuda, and T. Kato (2004), Space time distribution of afterslip following the 2003 Tokachi-oki earthquake: Implications for variations in fault zone frictional properties, *Geophys. Res. Lett.*, *31*, L06623, doi:10.1029/2003GL019410.

Mochizuki, K., et al. (2005), Intense PP reflection beneath the aseismic forearc slope of the Japan Trench subduction zone and its implication of aseismic slip subduction, *J. Geophys. Res.*, *110*, B01302, doi:10.1029/2003JB002892.

Nakanishi, A., A. J. Smith, S. Miura, T. Tsuru, and S. Kodaira (2004), Structural factors controlling the coseismic rupture zone of the 1973 Nemuro-oki earthquake, the southern Kuril Trench seismogenic zone, *J. Geophys. Res.*, *109*, B05305, doi:10.1029/2003JB002574.

Nanayama, F., K. Satake, R. Furukawa, K. Shimokawa, B. F. Atwater, K. Shigeno, and S. Yamaki (2003), Unusually large earthquakes inferred from tsunami deposits along the Kuril trench, *Nature*, *424*, 660–663, doi:10.1038/nature01864.

Pelayo, A. M., and D. A. Wiens (1992), Tsunami earthquakes: Slow thrust-faulting event in the accretionary wedge, *J. Geophys. Res.*, *97*(B11), 15,321–15,337, doi:10.1029/92JB01305.

Satake, K., and Y. Tanioka (1999), Sources of tsunami and tsunamigenic earthquakes in subduction zones, *Pure Appl. Geophys.*, *154*, 467–483, doi:10.1007/s000240050240.

Satake, K., and S. Yamaki (2005), Tsunami source regions of the Tokachi-oki and Nemuro-oki earthquakes between 19th and 21th centuries [in Japanese], *Earth Mon.*, *49*, 168–172.

Sato, H., et al. (2005), Earthquake source fault beneath Tokyo, *Science*, *309*(5733), 462–464, doi:10.1126/science.1110489.

Schwartz, S. Y., and L. J. Ruff (1987), Asperity distribution and earthquake occurrence in the southern Kuril Island arc, *Phys. Earth Planet. Inter.*, *49*, 54–77, doi:10.1016/0031-9201(87)90132-4.

Shinohara, M., et al. (2008), Precise aftershock distribution of the 2007 Chuetsu-oki Earthquake obtained by using an ocean bottom seismometer network, *Earth Planets Space*, *60*, 1121–1126.

Shinohara, M., et al. (2011), Aftershock observation of the 2011 off the Pacific coast of Tohoku Earthquake by using ocean bottom seismometer network, *Earth Planets Space*, *63*, 835–840, doi:10.5047/eps.2011.05.020.

Simon, M., H. Gebrande, and M. Bopp (1996), Pre-stack migration and true-amplitude processing of DEKORP near-normal incidence and wide-angle reflection measurements, *Tectonophysics*, *264*, 381–392, doi:10.1016/S0040-1951(96)00138-2.

Takahashi, N., S. Kodaira, T. Tsuru, J. Park, Y. Kaneda, K. Suyehiro, H. Kinoshita, S. Abe, M. Nishino, and R. Hino (2004), Seismic structure and seismogenesis off Sanriku region, northeastern Japan, *Geophys. J. Int.*, *159*, 129–145, doi:10.1111/j.1365-246X.2004.02350.x.

Tanioka, Y., and K. Satake (1996), Fault parameters of the 1896 Sanriku tsunami earthquake estimated from tsunami numerical modeling, *Geophys. Res. Lett.*, *23*, 1549–1552, doi:10.1029/96GL01479.

Tanioka, Y., and T. Seno (2001), Sediment effect on tsunami generation of the 1896 Sanriku tsunami earthquake, *Geophys. Res. Lett.*, *28*(17), 3389–3392, doi:10.1029/2001GL013149.

Tanioka, Y., K. Hirata, R. Hino, and T. Kanazawa (2004), Slip distribution of the 2003 Tokachi-oki earthquake estimated from tsunami waveform inversion, *Earth Planets Space*, *56*, 373–376.

Tsujino, T. (2010), Dive report of "Shinkai 6500" at a middle part of upper reaches of the Kushiro Submarine Canyon, off Tokachi, Hokkaido, Japan, *Bull. Geol. Surv. Jpn.*, *61*(3–4), 125–136.

Tsuru, T., J. Park, S. Miura, S. Kodaira, Y. Kido, and T. Hayashi (2002), Along-arc structural variation of the plate boundary at the Japan Trench margin: Implication of interplate coupling, *J. Geophys. Res.*, *107*(B12), 2357, doi:10.1029/2001JB001664.

Tsuru, T., S. Miura, J. Park, A. Ito, G. Fujie, Y. Kaneda, T. No, T. Katayama, and J. Kasahara (2005), Variation of physical properties beneath a fault observed by a two-ship seismic survey off southwest Japan, *J. Geophys. Res.*, *110*, B05405, doi:10.1029/2004JB003036.

Wessel, P., and W. H. F. Smith (1991), Free software helps map and display data, *Eos Trans. AGU*, *72*(41), 441, doi:10.1029/90EO00319.

White, R. S., D. McKenzie, and R. K. O'Nions (1992), Oceanic crustal thickness from seismic measurements and rare earth element inversion, *J. Geophys. Res.*, *97*(B13), 19,683–19,715, doi:10.1029/92JB01749.

Yamanaka, Y., and M. Kikuchi (2002), Characteristic behavior of asperities, paper presented at Japan Earth and Planetary Science Joint Meeting, Seismol. Soc. of Jpn., Tokyo.

Yamanaka, Y., and M. Kikuchi (2003), Source process of the recurrent Tokachi-oki earthquake on September 26, 2003, inferred from teleseismic body waves, *Earth Planets Space*, *55*, e21–e24.